Duhan Surender[1,2], Chandra Mohan[1], Rakesh Kumar[2]

[1]K. R. Mangalam University, Gurugram - 122103, Haryana, India.
[2]Maharaja Surajmal Institute of Technology (GGSIPU), Janakpuri, New Delhi-110058, India

Scientific paper
ISSN 0351-9465, E-ISSN 2466-2585
https://doi.org/10.5937/zasmat2304503S

Zastita Materijala 64 (4)
503 - 511 (2023)

Novel modification of activated charcoal sheet with N-methylpolypyrrole and silver nanoparticles for removal of hexavalent chromium in water treatment processes

ABSTRACT

The novel NPPY-AgNP's@AC CPN were synthesized and used for batch mode reductive adsorption of hexavalent Chromium (Cr^{+6}) ions in water treatment processes. The Activated Charcoal (AC) sheet was firstly encapsulated with silver nanoparticles (AgNP's) by in-situ reduction method and capped with N-methylpolypyrrole (NPPY) to obtain NPPY-AgNP's@AC conducting polymer nanocomposites (CPN). The obtained CPN were characterized by HR-FESEM, XRD, FTIR, and EDS. The nanocomposite materials showed excellent Cr^{+6} ions adsorption efficiency (Ad%) of 97.8% with adsorption capacity (qe) of 340 mg/g. The impact of various parameters like pH, adsorbent dose, initial Cr^{+6} ions concentration, temperature, and contact time on Ad% and qe were evaluated. The recycling experiments of NPPY-AgNP's@AC CPN revealed their enhanced reuse performance and could be utilised for five consecutive cycles without suffering much reductions in their initial efficacy. The novel PPY-AgNP's@AC CPN seems to be highly efficient materials for Cr^{+6} ions removal from polluted water.

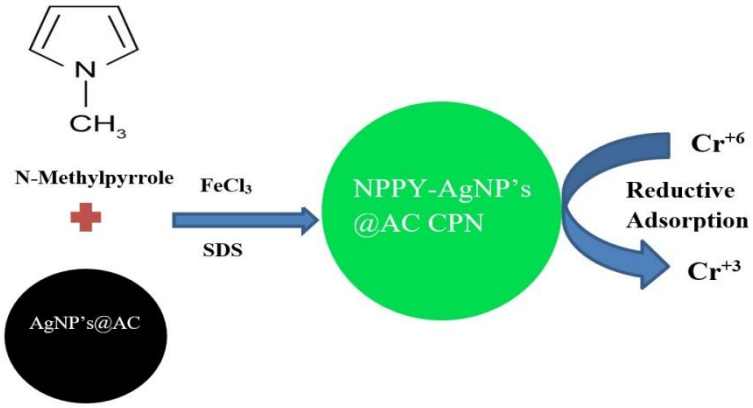

Figure 1. Graphical abstract

Slika 1. Graficki apstrakt

Keywords: *Heavy metal ions, activated charcoal, silver nanoparticles, N-methylpolypyrrole, hexavalent chromium*

1. INTRODUCTION

The heavy metals are released in to different aquatic environments directly or indirectly and raising concern in today's world because of their non-biodegradability, toxicity, mobility in ground water, and carcinogenicity [1]. The human body needs a limited amount of the heavy metals like Zn, Fe, Cr^{3+} ions, and Mn, which are considered micro-minerals. The presence of the heavy metals like Hg, As, Ni, Pb, Cd, Cu, Co and Cr^{6+} ions, in water, even in trace amounts, is always detrimental. Among the two forms of chromium in aqueous solution Cr^{+6} is most toxic form because of enhanced mobility and carcinogenic properties [2,3]. As per WHO guidlines, the permiscible limit for Cr^{+6} ions in industrial effluent water is 0.1 mg/L and in drinking water is 0.05 mg/L. The effective removal of Cr^{6+} ions from water is a critical issue of the present [4].

*Corresponding author: Rakesh Kumar
E-mail: rakeshkumar@msit.in
Paper received: 27.09. 2023.
Paper accepted: 15. 10. 2023.
Paper is available on the website: www.idk.org.rs/journal

To remove heavy metals from water, a number of techniques have been used, including precipitation, photocatalytic reduction, electrochemical treatment, and adsorption [5]. The most effective approach for removing organic and heavy metal pollutants from water is adsorption. The adsorption technique uses renewable resources, is inexpensive, and is eco-friendly [6].

The conducting polymer nanocomposites (CPN) have outstanding adsorptive performance against organic contaminants and heavy metal ions in water. Chauke et al. studied batch mode efficient removal of highly toxic Cr^{6+} ions from water utilizing novel PPY, Graphene oxide (GO) and alpha cyclodextrin (αCD) nanocomposite (GO-αCD-PPY NC) [7]. S. Li et al. evaluated batch mode removal of Cr^{6+}ions from water using bamboo-like PPY nanotubes [8]. Chen et al. examined efficient adsorption of Cr^{+6} ions from wastewater by utilizing PPY sugarcane bagasse (SCB) composites PPY@SCB [9]. Shao et al. synthesized bacterial cellulose (BC) and PPY composites (PPY@BC) having nanofiber microstructure and utilized for efficient removal of Cr^{+6} ions from water [10]. Sahu et al. synthesized flower like PPY and Cerium Phosphate ($CePO_4$) nanocomposite material (PPY-$CePO_4$) for adsorptive removal of Cr^{+6} ions in aqueous medium [11].

In the present work novel NPPY-AgNP's@AC CPN were prepared by encapsulating the AC sheet with AgNP's and capping with NPPY. The synthesized nanocomposites were investigated for their Cr^{+6} ions adsorption performance in aqueous solutions.

2. MATERIALS AND METHODS

2.1. Materials

N-methylpyrrole (CDH) was double distilled, $FeCl_3$ 99% pure, $AgNO_3$, isopropanol (Qualigens), sodium dodecyl sulfate (SDS) (CDH) were used as received and Activated Charcoal sheets were purchased from CHEMCO (Karol Bagh, New Delhi). $NaBH_4$, propan-2-ol and $K_2Cr_2O_7$, NaOH and HCl, (CDH) and buffer tablets were procured from PURO Chemicals (Tilak Nagar, New Delhi).

2.2. Methods

2.2.1. Preparation of NPPY capped - AC sheet (NPPY@AC)

The dry, blank AC sheet was kept in Propan-2-ol (20%) for 20 minutes. The AC sheet was then dried and maintained at 4°C till usage after being rinsed three times in DIN water [12]. The N-methylpyrrole (NPY) monomer was polymerized by in-situ oxidative suspension polymerization in the presence of $FeCl_3$ as an oxidant while maintaining a monomer to oxidant ratio of 1:2. The NPPY capped AC sheet that was subsequently acquired was cleaned in deionised water (DIN) and kept in vacuum oven at 50^{o}C for 8–10 hours.

2.2.2. Preparation of AgNP's encapsulated AC sheets capped with NPPY (NPPY-AgNP's@AC CPN)

The sheets were prepared in two steps:

2.2.3. Encapsulation of AC sheet with AgNP's to obtain AgNP's@AC:

The propan-2-ol treated AC sheets were encapsulated with AgNP's by in-situ reduction of 5-mM aqueous $AgNO_3$ with 5 mM aqueous $NaBH_4$ solution [12]. The AgNP's encapsulated AC sheet so obtained was rinsed with DIN water for 10 seconds and dried in vacuum oven at 50^{o}C for 8-10 hrs.

2.2.4. Capping of AgNP's encapsulated AC sheet with NPPY to obtain NPPY-AgNP's@AC CPN:

The capping of AgNP's@AC with NPPY to obtain NPPY-AgNP's@AC CPN was carried by same methodology as we capped blank AC sheet with NPPY.

2.3. Characterization

2.3.1. HR-FESEM analysis

The electron microscopy of all the samples was accomplished by using HR-FESEM coupled with EDS (JEOL). The Fig. 2 (b) clearly shows globular microstructures of NPPY formed on to AC sheet, Fig. 2 (c) provides evidence of encapsulation of AC sheet with AgNP's, which is further supported by EDS in Fig. 3(b) while Fig. 2 (d) reveals capping of globular microstructures of NPPY on to AC@AgNP's.

Table 1. Blank AC EDS eZAF Quant Results- Analysis uncertainty:12.30%

Tabela 1. Prazan AC EDS eZAF Quant Results- Neizvesnost analize: 12,30%

Element	Weight%	Atomic%	Error%	R	A	F
C (K)	70.7	79.1	9.7	0.9256	0.1343	1.0000
O (K)	24.5	20.5	10.8	0.9345	0.0509	1.0000
Au (L)	4.9	0.3	9.2	0.9910	0.9974	1.0630

Table 2. AgNP's@AC EDS eZAF Quant Results- Analysis uncertainty: 28.85%

Tabela 2. AgNP's@AC EDS eZAF Quant Results- Neizvesnost analize: 28,85%

Element	Weight%	Atomic%	Error%	R	A	F
C (K)	75.4	83.0	9.7	0.9286	0.1373	1.0000
O (K)	20.2	16.7	10.9	0.9372	0.0542	1.0000
Ag (L)	0.9	0.1	5.1	0.9654	0.8852	1.0055
Au (L)	3.4	0.2	10.7	0.9915	0.9978	1.0696

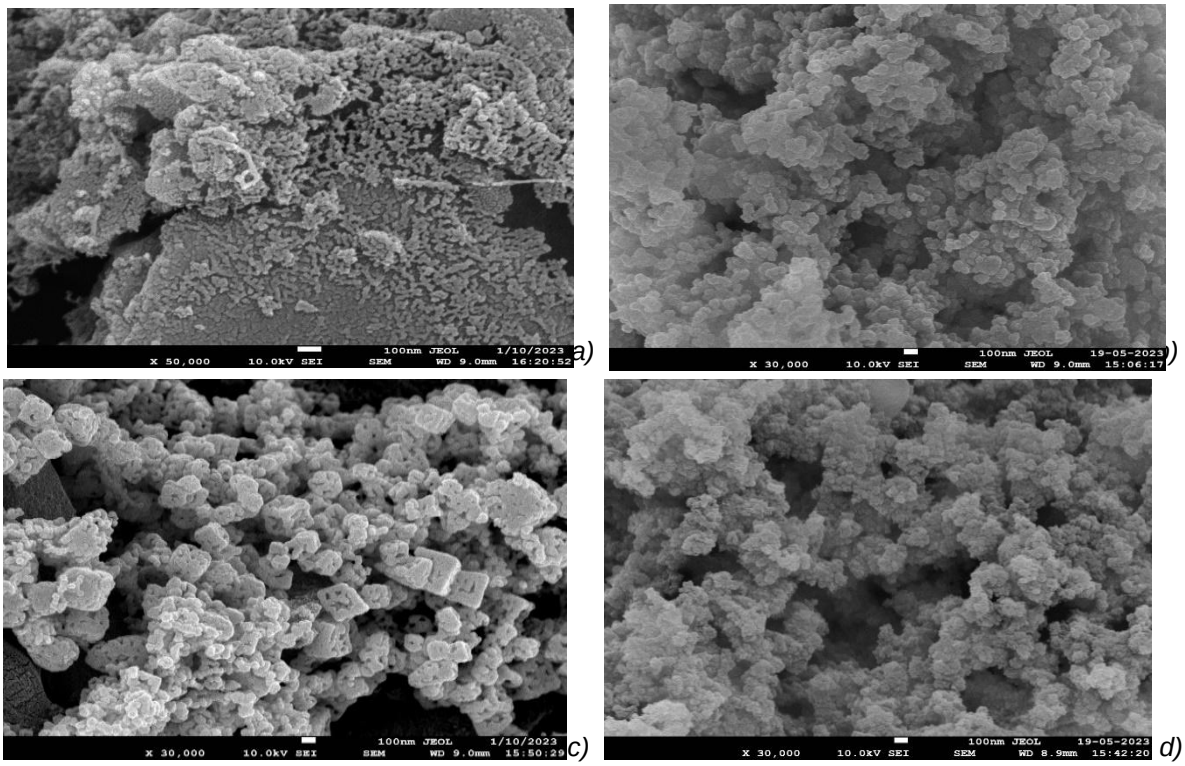

Figure 2. HR-FESEM images of (a) Blank AC sheet (b) NPPY@AC (c) AgNP's@AC (d) NPPY-AgNP's@AC CPN.

Slika 2. HR-FESEM slike (a) Prazan AC list (b) NPPI@AC (c) AgNP's@AC (d) NPPI-AgNP's@AC CPN

2.3.2. EDS analysis

The Fig. 3 shows EDS spectrum of blank AC sheet (a) and AgNP's@AC (b) respectively and presence of distinct silver peak in AgNP's@AC affirms loading of AgNP's on to AC. The eZAF Quant Results are given in table1 for blank AC and table 2 for AgNP's@AC.

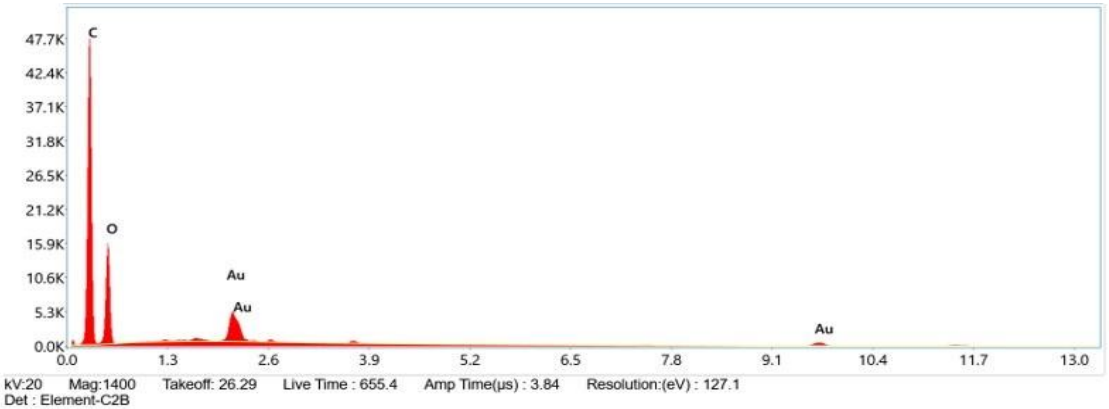

a)

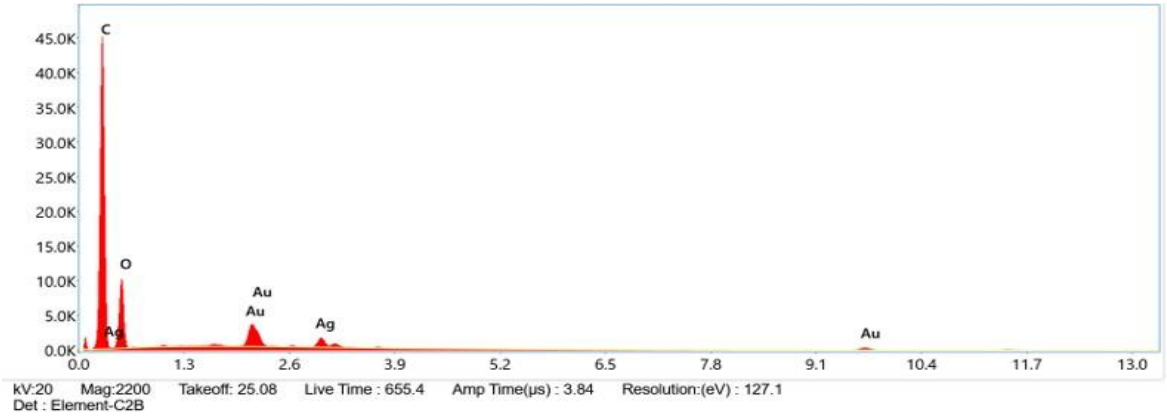

b)

Figure 3. EDS images of (a) Blank AC (b) AgNP's@AC

Slika 3. EDS slike (a) Prazan AC (b) AgNP's@AC

2.3.3. FTIR analysis

The FTIR analysis of the samples were carried out using Perkin Elmer Spectrometer Version 10.6.2 (Fig. 4).

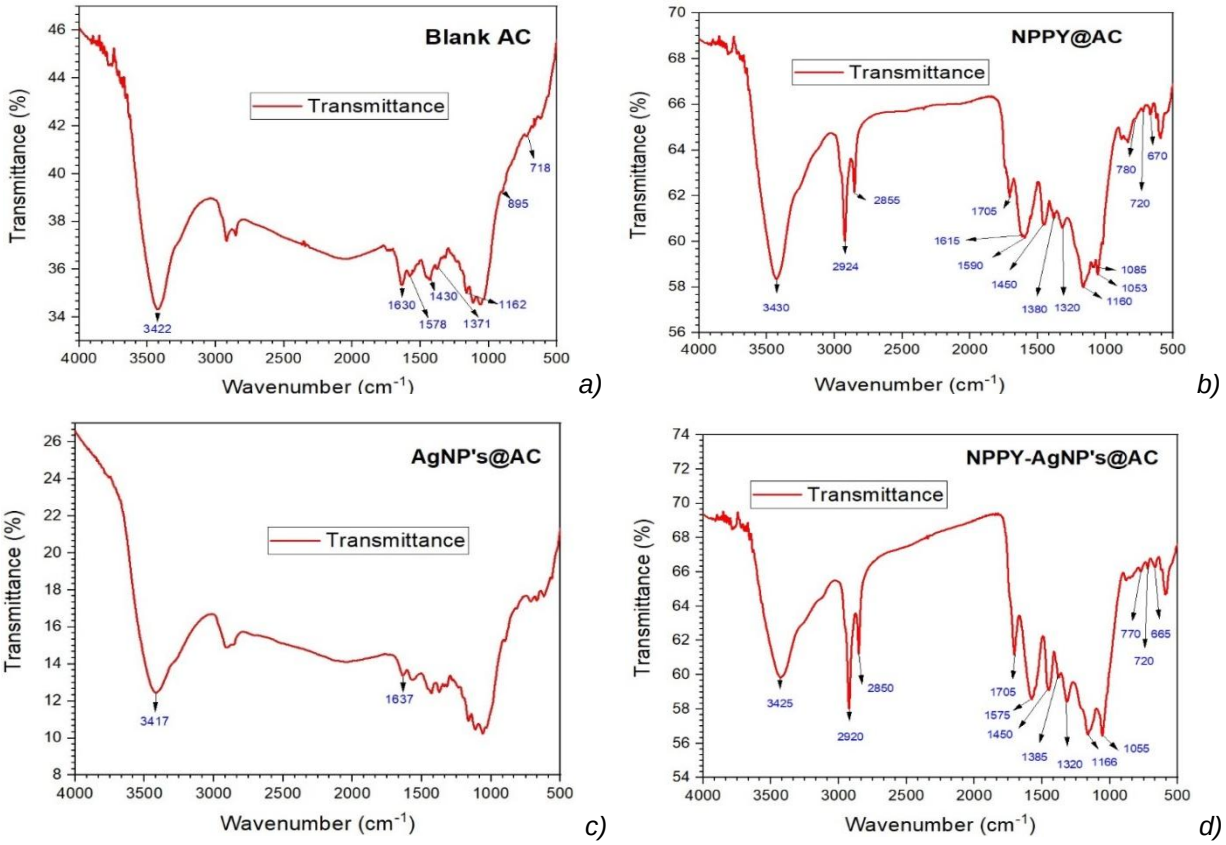

Figure 4. FTIR images of (a) Blank AC sheet (b) NPPY@AC (c) AgNP's@AC (d) NPPY-AgNP's@AC

Slika 4. FTIR slike (a) praznog AC lista (b) NPPI@AC (c) AgNP's@AC (d) NPPI-AgNP's@AC

The FTIR spectrum of NPPY@AC and NPPY-AgNP's@AC shows bands at 3425 and 2530 cm^{-1} (ring C-H stretching), 2950 and 2920 cm^{-1} (asymmetric and symmetric methyl C-H stretching), 1705 cm^{-1} (stretching of carbonyl groups), 1590 and 1575 cm^{-1} (interring C-C vibrations and intraring C=C vibrations), 1450, 1380 and 1320 cm^{-1}, (C-N vibrations and C-H deformations), and 1160, 1085, 1053 cm^{-1} and bands at 780, 720 and 670 cm^{-1} from C–H deformations and -CH_3 rocking [12/15] A little bit shift in IR value of NPPY-AgNP's@AC CPN can be attributed nature of

interactions among different components of CPN material.

2.3.4 XRD analysis

The Fig. 5 (c) shows XRD pattern of AgNP's@AC shows the peaks at (2θ) as 38.06° (111), 42.68° (200), 64.26° (220) and 77.32° (311) with corresponding planes. The mean crystalline particle size of the AgNP's was estimated 20 nm using the width of (111) Bragg's reflection. X-ray diffraction analysis of NPPY@AC showed broad characteristic peak for amorphous NPPY peak at about 2θ = 22.5° (Fig. 5 (b)). The mean particle size for NPPY was determined using Debye-Scherer equation (Eq. 1) and found to be 60 nm.

$$d = K\frac{\lambda}{\beta \cos \emptyset} \quad (1)$$

where, d is the average diameter of crystallite, K is shape constant (0.9), λ is radiation wavelength (1.54 Å), β is full width at half maxima, ∅ is Bragg's angle of respective peaks. The Blank AC sheet (Fig. 5 (a)) and NPPY-AgNP's@AC (Fig. 5 (d)) samples showed XRD peaks at 22° and 23° respectively revealing their amorphous [16].

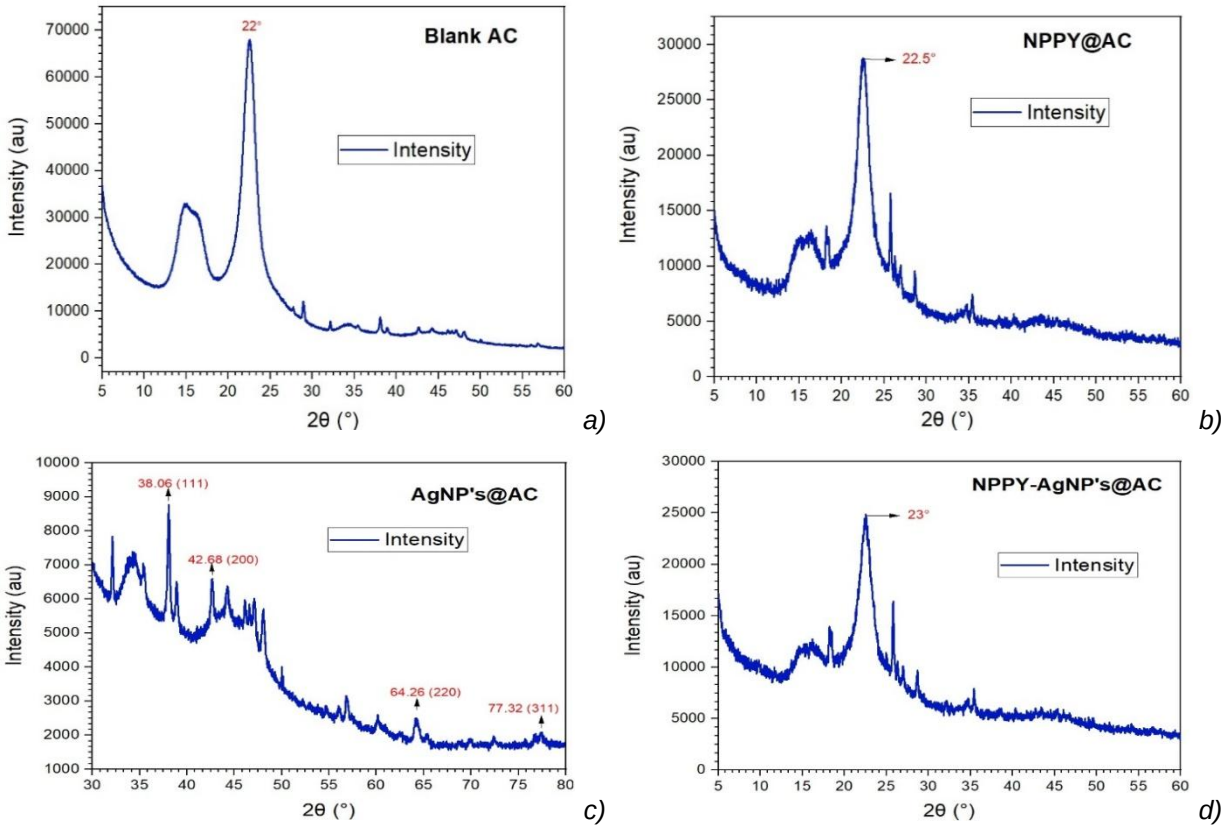

Figure 5. XRD images of (a) Blank AC sheet (b) NPPY@AC (c) AgNP's@AC (d) NPPY-AgNP's@AC

Slika 5. XRD slike (a) Prazan AC list (b) NPPI@AC (c) AgNP's@AC (d) NPPI-AgNP's@AC

3. RESULTS & DISCUSSION

3.1. Adsorption studies

All the adsorption studies of Cr^{+6} ions were carried in batch mode and with determination of the concentration of the Cr^{+6} ions using of UV-Vis spectroscopy (UV-1700 PharmaSpec, Shimadzu). The Cr^{+6} ions aqueous solutions were prepared with initial concentration of 25 mg/L and adjusted the pH range from 2 to 10. The interaction was allowed at room temperature for 24 hours, with agitation using orbital shaker at 300 rpm. The maximum absorbance wavelength (λ_{max}) for Cr^{+6} ions was determined to be 355 nm. The absorbance of the solution was measured before and after the adsorption process.

The adsorption efficiency of PPY-AgNP's@AC sheet was calculated in terms of adsorption % (Ad%) and adsorption capacity (q_e) in mg/ g using following relations (Eq. 1 & 2):

$$Ad\% = \frac{C_o - C_f}{C_0} \times 100 \quad (2)$$

Where: C_0 - Initial concentration (mg/L) of Cr^{+6} ions in water and C_f - Final concentration (mg/L) of Cr^{+6} ions in water.

$$q_e = \frac{V(C_o - C_e)}{m} \quad (3)$$

where:

V - Volume of Cr^{+6} ions solution used,

C_e - Cr^{+6} ions concentration (mg/L) at equilibrium,

m - Mass of adsorbent used.

3.2. Effect of various parameters on adsorption of Cr^{+6} ions

3.2.1. pH:

The pH of aqueous solution significantly affects the Ad% by determining the adsorbent surface charge and enhances adsorbate and the adsorbent interactions. The sharp decline in Ad% of Cr^{+6} ions with increase in pH (under alkaline conditions) is due to substitution of intercalated chloride ions (Cl^-) of NPPY by hydroxide ions (^-OH). The Fig. 6 (a), shows the variation of Ad% as a function of the pH and in all cases, the NPPY-AgNP's@AC sheet exhibited the highest Ad% at pH 2.

3.2.2. Effect of contact time

The Fig. 6 (b) shows variation in Ad% with contact time of the NPPY-AgNP's@AC sheet with Cr^{+6} ions. In the first 15 min. the Ad% increases sharply and maximum Ad% at 20 min. and reaches to saturation limit in short time and was observed up to 60 min. (although no change up to 140 min.). This behaviour may be explained by first having a large number of reactive sites available on the adsorbent surface, which then get saturated as contact duration grows until an equilibrium is reached and no further significant change occurs.

3.2.3. Effect of initial Cr^{+6} ions concentration

The Fig. 6 (c) shows how Ad% vary with increase of initial concentration of Cr^{+6} ions in aqueous solution. The Ad% decreased with an increase in the initial concentration of Cr^{+6} ions. The comparative decline in the number of active sites on the adsorbent surface with the advancement of the adsorption process results in the decline in Ad%.

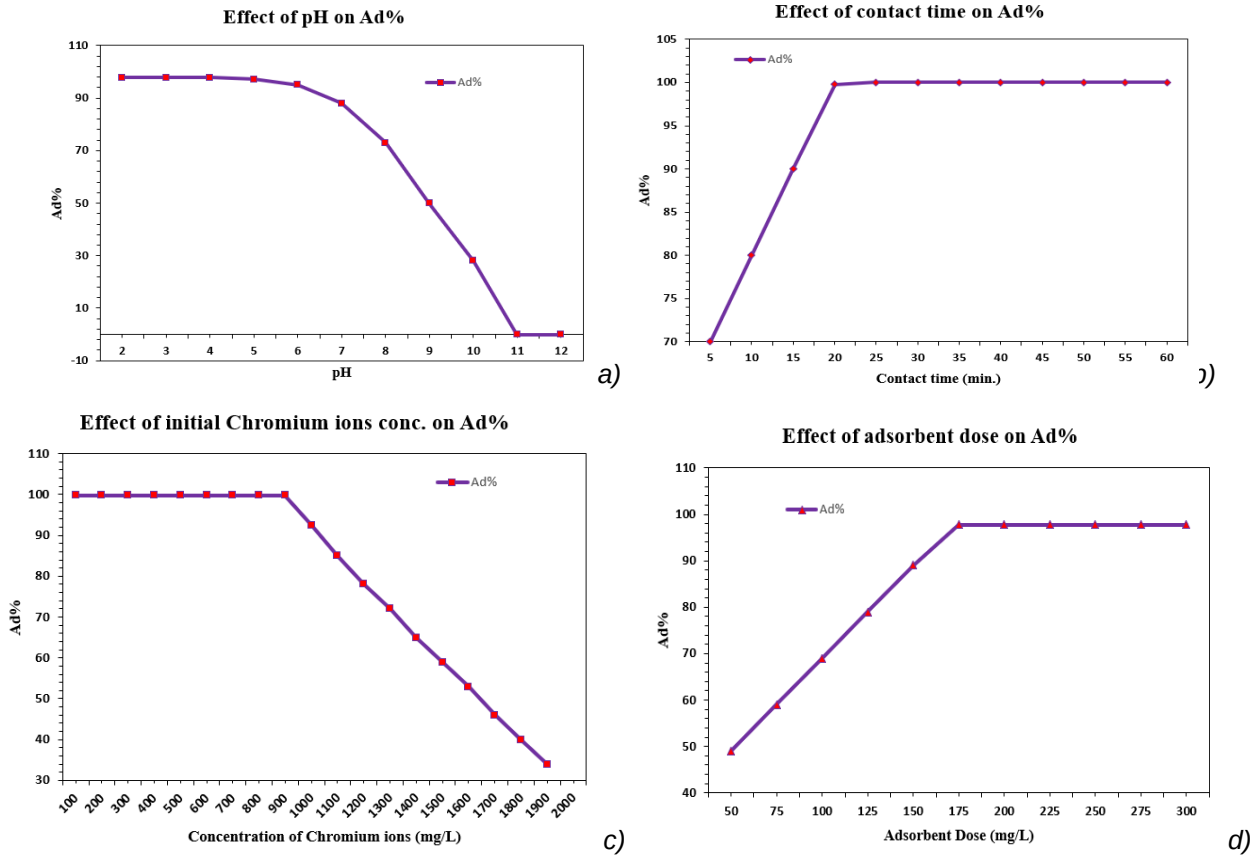

Figure 6. Effect of (a) pH (b) contact time (min.) (c) initial Chromium ions concentration (d) adsorbent dose on adsorption of Cr^{+6} ions

Slika 6. Uticaj (a) pH (b) vremena kontakta (min.) (c) početne koncentracije jona hroma (d) doze adsorbenta na adsorpciju Cr^{+6} jona

3.2.4. Effect of adsorbent dose

The dose of NPPY-AgNP's@AC significantly influences Ad% via increasing adsorption surface area. The Fig. 6 (d) represents variation in Ad% as a function of adsorbent dose and the highest Ad% at 175 mg of adsorbent dose was observed.

3.2.5. Effect of temperature

The Fig. 7 (a) shows variation in *qe* with increase in temperature of adsorption process from 275 K to 325 K. The significant increase in *qe* values with rise in temperature was observed as a result of endothermic adsorption process.

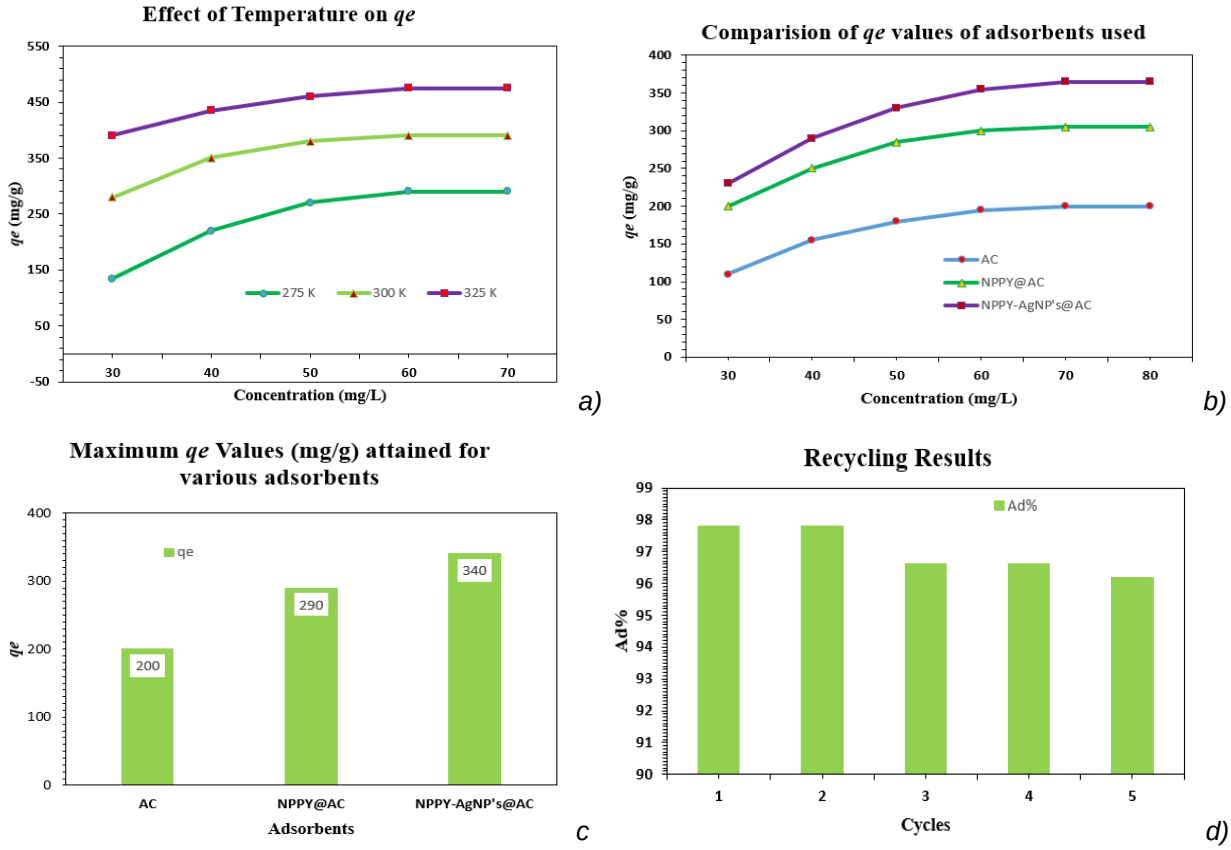

Figure 7. Effect of (a) Temperature on qe (b) Ad% comparison of various adsorbents (c) Maximum qe values for various adsorbents (d) Recycling results

Slika 7. Uticaj (a) Temperature na qe (b) Ad% poređenje različitih adsorbenata (c) Maksimalne vrednosti qe za različite adsorbente (d) Rezultati reciklaže

3.3. Mechanism of adsorption

The Cr^{+6} ions are present in aqueous solution as negatively charged ions ($Cr_2O_7^{2-}$ and $HCrO^{4-}$), the probable mechanism for their adsorption involves protonation of NPPY in an acidic medium to acquire positive charged groups (NH_2^+ groups), and electrostatic force thus increases the efficiency of adsorption. Additionally, chelation of Cr^{+3} to NPPY polymeric chains is favoured by the reduction of Cr^{+6} to Cr^{+3} by NPPY chains and AgNP's. Because of this, electrostatic interactions are encouraged, increasing Ad%. However, the decrease in Ad% with increase in pH values beyond pH 6 is explained by the phenomenon of deprotonation of the NH_2^+ groups and increase in $^-$OH ions concentration. This cause reduction in number of reactive sites and $Cr_2O_7^{2-}$ and $HCrO_4^-$ must compete for reactive sites with $^-$OH ions, hence increased the electrostatic repulsive forces [17]. The encapsulation of AC with AgNP's probably increased the reduction of Cr^{+6} to Cr^{+3} and hence enhanced performance of NPPY-AgNP's@AC CPN sheets as compared to NPPY@AC and blank AC [18-20].

3.4. Reuse experiments

The reusability of NPPY-AgNP's@AC CPN sheets were investigated under ideal conditions of pH 2, concentration (50 or 25 mg/L) and interaction time (50, 75 and 140 min) for adsorption of Cr^{+6} ions. The exhausted NPPY-AgNP's@AC CPN sheet was placed in beaker containing 10 mL of a

0.1 M NaOH (0.1 M SDS) solution and agitated for 30 min. at 300 rpm. The CPN sheet was washed with DIN water and used again for another cycle of adsorption of Cr^{+6} ions. The NPPY-AgNP's@AC CPN sheet showed promising results up to five consecutive reuse cycles (Fig. 7 (d).

4. CONCLUSIONS

The NPPY-AgNP's@AC CPN sheet was prepared by in-situ reduction of aqueous $AgNO_3$ solution with aqueous $NaBH_4$ solution to obtain AgNP's on to AC sheet (AgNP's @AC) and subsequent capping of NPPY on to AgNP's@AC. Excellent Cr^{+6} ions Ad% of 97.8% and the *qe* of 340 mg/g were displayed by the NPPY-AgNP's@AC sheet. In comparison to NPPY@AC and blank AC sheet, the encapsulation of AC with AgNPs was found to improve Cr^{+6} to Cr^{+3} reduction and have improved adsorption capability. The NPPY-AgNP's@AC CPN sheet was reused up to five times in a row without suffering appreciable Ad% and qe value losses. This type of hybrid material utilization is a desirable alternative solution for effluent water remediation contaminated with Cr^{+6} ions.

Acknowledgements

This study was not possible without kind support of K.R. Mangalam University, Gurugram, India-122130, National Physical Laboratory (NPL), New Delhi-110012 and Maharaja Surajmal Institute of Technology (MSIT), New Delhi-110058, India. We are highly thankful to these organizations.

5. REFERENCES

[1] C.M.Cooper (1993) Biological Effects of Agriculturally Derived Surface Water Pollutants on Aquatic Systems—A Review, J. Environ. Qual., 22(3), 402–408.

[2] Z.Fu, S.Xi (2020) The effects of heavy metals on human metabolism, Toxicol. Mech. Methods, 30(3), 167–176.

[3] S.Chowdhury, M.Mazumder, J.Al-Attas, T.Husain, (2016) Heavy metals in drinking water: Occurrences, implications, and future needs in developing countries, Sci. Total Environ., 569–570, 476–488.

[4] Documents (2012) WHO Chemical Safety - Activity Report, 78, 1–18.

[5] I.Ihsanullah, M.Atieh, M.Sajid, M.Nazal (2021) Desalination and environment: A critical analysis of impacts, mitigation strategies, and greener desalination technologies, Sci. Total Environ., 780,146585.

[6] D.Sud, G.Mahajan, M.Kaur (2008) Agricultural waste material as potential adsorbent for sequestering heavy metal ions from aqueous solutions - A review, Bioresour. Technol., 99(14), 6017–6027.

[7] V.P.Chauke, A.Maity, A.Chetty (2015) High-performance towards removal of toxic hexavalent chromium from aqueous solution using graphene oxide-alpha cyclodextrin-polypyrrole nanocompo-sites, Elsevier-Journal Mol. Liq., 211, 71–77.

[8] S.Li et al. (2012) Preparation of bamboo-like PPy nanotubes and their application for removal of Cr (VI) ions in aqueous solution, J.Colloid Interface Sci., 378(1), 30–35.

[9] Z.Chen, K.Pan (2021) Enhanced removal of Cr(VI) via in-situ synergistic reduction and fixation by polypyrrole/sugarcane bagasse composites, Chemosphere, 272, 129606.

[10] Y.Shao, Z.Fan, M.Zhong, W.Xu, C.He, Z.Zhang (2021) Polypyrrole/bacterial cellulose nanofiber composites for hexavalent chromium removal," Cellulose, 28(4), 2229–2240.

[11] S.Sahu, N.Bishoyi, R.K.Patel (2021) Cerium phosphate polypyrrole flower like nanocomposite: A recyclable adsorbent for removal of Cr(VI) by adsorption combined with in-situ chemical reduction, J. Ind. Eng. Chem., 99, 55–67.

[12] M.Ben-Sasson et al. (2014) In situ formation of silver nanoparticles on thin-film composite reverse osmosis membranes for biofouling mitigation, Water Res., 62, 260–270.

[13] M.I.Redondo, E.De la Sánchez Blanca, M.García, M.A.Raso, J.Tortajada, M.González-Tejera (2001) FTIR study of chemically synthesized poly(N-methylpyrrole)," Synth. Met.,122,(2), 431–435.

[14] A.Saidfar, M.Alizadeh, S.Pirsa (2020) Application of Nano-sized Poly (N-methyl pyrrole-pyrrole) Fiber to the Headspace Solid-Phase Microextraction of Volatile Organic Compounds from Yogurt, J. Chem. Lett, 1, 39–46.

[15] A.Khan, A.A.Khan, I.Khan, A.Asiri, M.Rahman (2022) Sol-Gel Synthesis and Characterization of Highly Selective Poly(N-methyl pyrrole) Stannous(II)Tungstate Nano Composite for Mercury (Hg(II)) Detection, Crystals, 12(3), 1-14.

[16] M.Chougule, S.Pawar, P.Godse, R.Mulik, S. Sen, V.Patil (2011) Synthesis and Characterization of Polypyrrole (PPy) Thin Films," Soft Nanosci. Lett., 01(01), 6–10.

[17] W.Liu et al. (2018) Efficient removal of hexavalent chromium from water by an adsorption-reduction mechanism with sandwiched nanocomposites, RSC Adv., 8(27),15087–15093.

[18] Z.H.Farooqi, M.W.Akram, R.Begum, W.Wu, A.Irfan (2020) Inorganic nanoparticles for reduction of hexavalent chromium: Physicochemical aspects," J. Hazard. Mater., 402,123535.

[19] Y.Chen, S.Ji, C.Chen, Q.Peng, D.Wang, Y.Li (2018) Single-Atom Catalysts: Synthetic Strategies and Electrochemical Applications, Joule, 2(7), 1242–1264.

[20] X.Fei et al. (2016) Biochar-based nano-composites for the decontamination of wastewater: A review, Bioresour. Technol., 212, 318–333.

IZVOD

NOVA MODIFIKACIJA LISTA AKTIVNOG UGLJA SA N-METILPOLIPIROLOM I NANOČESTICAMA SREBRA ZA UKLANJANJE HEKSAVALENTNOG HROMA U PROCESIMA TRETMANA VODE

Novi NPPI-AgNP's@AC CPN su sintetizovani i korišćeni za serijsku reduktivnu adsorpciju heksavalentnih jona hroma (Cr^{+6}) u procesima prečišćavanja vode. List sa aktivnim ugljem (AC) je prvo kapsuliran sa nanočesticama srebra (AgNP) metodom redukcije na licu mesta i zatvoren sa N-metilpolipirolom (NPPI) da bi se dobili NPPI-AgNP @AC provodljivi polimerni nanokompoziti (CPN). Dobijeni CPN su okarakterisani pomoću HR-FESEM, XRD, FTIR i EDS. Nanokompozitni materijali su pokazali odličnu efikasnost adsorpcije jona Cr^{+6} (Ad%) od 97,8% sa kapacitetom adsorpcije (qe) od 340 mg/g. Ocenjen je uticaj različitih parametara kao što su pH, doza adsorbenta, početna koncentracija Cr+6 jona, temperatura i vreme kontakta na Ad% i qe. Eksperimenti recikliranja NPPI-AgNP's@AC CPN-a su otkrili njihove poboljšane performanse ponovne upotrebe i mogli su da se koriste u pet uzastopnih ciklusa bez mnogo smanjenja njihove početne efikasnosti. Čini se da je novi PPI-AgNP's@AC CPN visoko efikasan materijal za uklanjanje Cr^{+6} jona iz zagađene vode.

Ključne reči: *Joni teških metala, aktivni ugalj, nanočestice srebra, N-metilpolipirol, heksavalentni hromr*

Naučni rad
Rad primljen: 27.09.2023.
Rad prihvacen: 15.10.2023.
Rad je dostupan na sajtu: www.idk.org.rs/casopis